

Dopamine-Deprived Striatal GABAergic Interneurons Burst and Generate Repetitive Gigantic IPSCs in Medium Spiny Neurons

Nathalie Dehorter,¹ Celine Guigoni,² Catherine Lopez,¹ June Hirsch,¹ Alexandre Eusebio,¹ Yehezkel Ben-Ari,¹ and Constance Hammond¹

¹Institut de Neurobiologie de la Méditerranée Unité Mixte de Recherche (UMR) 901, Inserm and Aix Marseille II University, 13009 Marseille, France, and

²Centre National de la Recherche Scientifique UMR 5227, Université Bordeaux 2, 33076 Bordeaux, France

Striatal GABAergic microcircuits modulate cortical responses and movement execution in part by controlling the activity of medium spiny neurons (MSNs). How this is altered by chronic dopamine depletion, such as in Parkinson's disease, is not presently understood. We now report that, in dopamine-depleted slices of the striatum, MSNs generate giant spontaneous postsynaptic GABAergic currents (single or in bursts at 60 Hz) interspersed with silent episodes, rather than the continuous, low-frequency GABAergic drive (5 Hz) observed in control MSNs. This shift was observed in one-half of the MSN population, including both "D₁-negative" and "D₁-positive" MSNs. Single GABA and NMDA channel recordings revealed that the resting membrane potential and reversal potential of GABA were similar in control and dopamine-depleted MSNs, and depolarizing, but not excitatory, actions of GABA were observed. Glutamatergic and cholinergic antagonists did not block the GABAergic oscillations, suggesting that they were generated by GABAergic neurons. In support of this, cell-attached recordings revealed that a subpopulation of intrastriatal GABAergic interneurons generated bursts of spikes in dopamine-deprived conditions. This subpopulation included low-threshold spike interneurons but not fast-spiking interneurons, cholinergic interneurons, or MSNs. Therefore, a population of local GABAergic interneurons shifts from tonic to oscillatory mode when dopamine deprived and gives rise to spontaneous repetitive giant GABAergic currents in one-half the MSNs. We suggest that this may in turn alter integration of cortical signals by MSNs.

Introduction

The striatum plays a central role in movement elaboration, most notably by integrating the converging glutamatergic inputs from the neocortex. The GABAergic medium spiny projection neurons (MSNs) that constitute 95% of all striatal neurons provide the only output of the striatum and are the final step of this integration process. Local GABAergic and cholinergic interneurons represent the remaining 5%. The striatal network is controlled by dopaminergic synapses, whose loss in Parkinson's disease leads to major motor deficits. The manner by which dopamine controls the operation of the striatal network is not yet understood. In contrast to the extensive investigations performed on the fate of spontaneous or evoked glutamatergic currents (PSCs) in dopamine (DA)-depleted MSNs (Calabresi et al., 2007) and despite

the overwhelming role of GABA microcircuits in the striatum (Wilson, 2007), little is known on the alterations of GABAergic currents under these conditions.

Two types of intrastriatal GABAergic interneurons control the activity of MSNs: fast-spiking (FS) interneurons and low-threshold spike (LTS) interneurons (Kawaguchi, 1993; Tepper and Bolam, 2004) that innervate the soma and proximal dendrites of MSNs (Kita et al., 1990; Bennett and Bolam, 1994; Kubota and Kawaguchi, 2000). They exert feedforward inhibition that prevents or delays the generation of action potentials (Plenz and Kitai, 1998; Koós and Tepper, 1999; Mallet et al., 2005; Gustafson et al., 2006). There is also a dense network of recurrent GABAergic synapses between MSNs, located on dendritic spines and shafts (Wilson and Groves, 1980). These provide lateral inhibition as a result of summation of the small amplitude IPSCs (Czubayko and Plenz, 2002; Tunstall et al., 2002; Venance et al., 2004; Tepper et al., 2008). Dopaminergic input from the substantia nigra modulates the activity of GABAergic interneurons via several presynaptic and postsynaptic dopamine receptor subtypes (Bracci et al., 2002; Momiyama, 2002; Centonze et al., 2002, 2003), as do cholinergic interneurons [the tonically active neurons (TANs)] (Zhou et al., 2002; Sullivan et al., 2008) via muscarinic and nicotinic receptors (Koós and Tepper, 2002).

Using the basal ganglia slice (BGS) (Beurrier et al., 2006) and slices of isolated striatum in which the striatum is deprived of its cortical and thalamic inputs, we now report that, in chronically

Received March 31, 2009; revised May 6, 2009; accepted May 6, 2009.

This work was supported by Inserm, Fondation de France, and Association France Parkinson. N.D. is supported by a PhD grant from the region Provence-Alpes-Côte d'Azur and the company Neuroservice. We thank Alfonso Represa, François Michel, Christophe Porcher, and Igor Medina for their help with immunocytochemical data.

Correspondence should be addressed to Constance Hammond, Institut de Neurobiologie de la Méditerranée Unité 901, Inserm, 163 route de Luminy, BP 13, 13273 Marseille Cedex 9, France. E-mail: hammond@inmed.univ-mrs.fr.

A. Eusebio's present addresses: Department of Neurology and Movement Disorders, Centre Hospitalier Universitaire Timone, 13385 Marseille, France; and Sobell Department of Motor Neuroscience and Movement Disorders, Institute of Neurology, Queen Square, London WC1N 3BG, UK.

DOI:10.1523/JNEUROSCI.1527-09.2009

Copyright © 2009 Society for Neuroscience 0270-6474/09/297776-12\$15.00/0

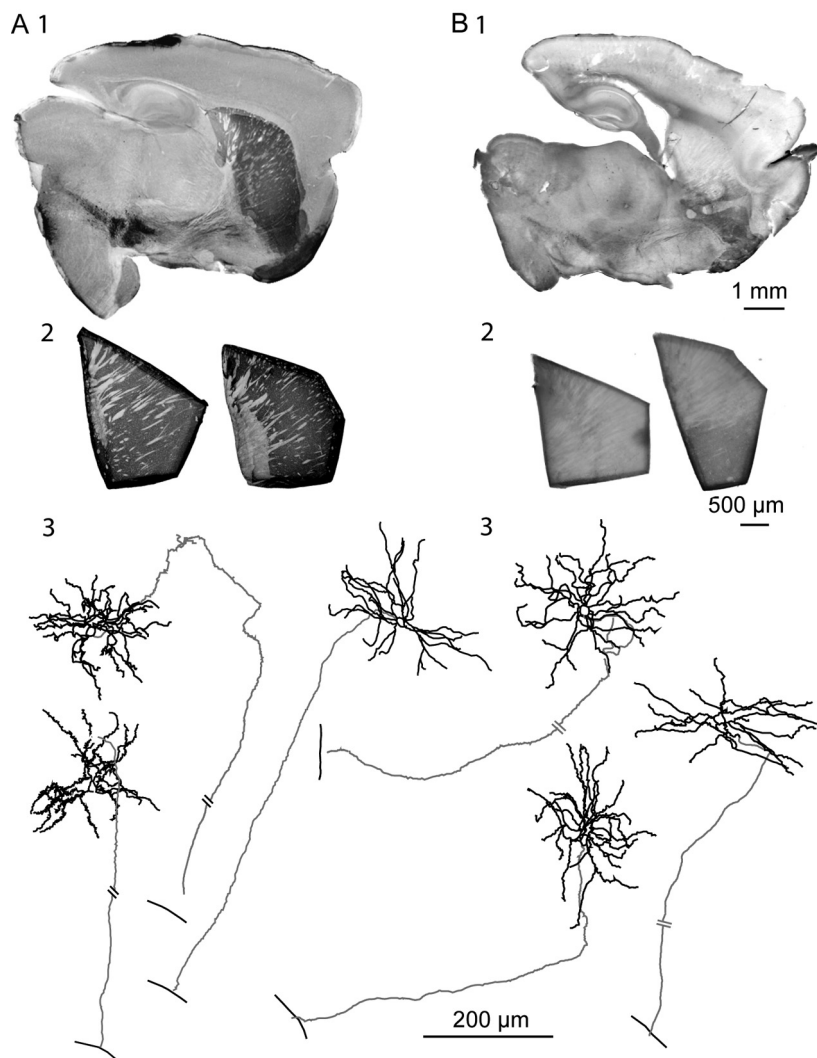


Figure 1. Extent of DA depletion in the striatum and identification of the recorded MSNs. TH immunohistochemistry of adult BGS (**1**) and isolated striatum (**2**) from control (**A**) and DA-depleted (**B**) mice. The striatum was isolated from the corresponding BGS before the recording session. Note the absence of dark TH labeling in the BGS (**B1**) and in the two isolated striatum (**B2**) from 6-OHDA-treated mice compared with the corresponding control ones (**A1, A2**). Neurolucida reconstruction of biocytin-filled MSNs recorded in control (**A3**) and DA-depleted (**B3**) isolated striatum is shown. Somas and dendritic trees are in black and axons are in gray. The single bars crossing the axons indicate GP boundary; the double bars indicate interruption in the drawing because of the length of the axon.

DA-depleted MSNs, the continuous activity of small amplitude GABAergic sPSCs is replaced in one-half of the MSN population by giant GABAergic events separated by silent episodes. These were not affected by nicotinic or muscarinic receptor antagonists. Cell-attached recordings of single GABA_A and NMDA channels from MSNs showed that this shift is not attributable to modifications of resting membrane potential (V_{rest}) or of the reversal potential for GABA (E_{GABA}). Nor did we find alterations of the spike threshold. Giant GABAergic currents are depolarizing but do not generate spikes in either control or DA-depleted MSNs. Chronic DA depletion did not affect the activity of MSNs (silent) or cholinergic interneurons (TANs, tonically active) or GABAergic FS interneurons (tonically active or silent) recorded in the cell-attached configuration *in vitro*. Rather, it led to remarkable intrinsic oscillations in a subpopulation of GABAergic LTS interneurons. We propose that the ensuing powerful GABAergic barrage of giant GABA sPSCs profoundly alters the integrative functions of the striatum by interacting with cortical information traveling throughout the striatum.

Materials and Methods

Chronic lesion of the dopaminergic innervation of the striatum. We lesioned the dopaminergic innervation in one striatum of C57BL/6 mice (15–25 g) aged postnatal day 15 (P15) to P50 by local stereotaxic injection of 6-hydroxydopamine (6-OHDA) under 5% ketamine (Imalgene 1000)/2.5% xylazine (Rompun 2%) anesthesia (10 μ l/g, i.p.). Two microinjections of 6-OHDA were performed through a NanoFIL syringe (outside diameter, 135 μ m; WPI) placed into the left dorsal striatum at the following coordinates using a David Kopf stereotaxic apparatus: 1.0 and 1.2 mm rostral to bregma, 1.8 and 2.2 mm lateral to the midline, 2.7 and 2.8 mm, respectively, below the surface of the skull. 6-OHDA was dissolved in saline containing 0.05% ascorbic acid, and injected at a dose of 6 μ g in a volume of 0.5 μ l over a 5 min period. The syringe was left in place for 5 min after the end of injection. We performed *in vitro* recordings 15–30 d after the lesion. The efficacy of the 6-OHDA-induced lesion of dopaminergic terminals in the striatum was determined 2–3 d before the recording session by apomorphine-induced rotation (0.5 mg/kg in 0.1% ascorbic acid, i.p.; Sigma-Aldrich) (Iancu et al., 2005). Lesioned mice performed 7.0 ± 0.3 right turns per minute and no left turn ($n = 47$). In contrast, control mice performed 0.18 ± 0.07 right turns per minute and 0.23 ± 0.06 left turns per minute ($n = 11$). We checked the extent of the lesion after the recording session by immunohistochemical visualization of tyrosine hydroxylase (TH) in the striatum (see below, Immunocytochemistry).

Slice preparation. C57BL/6 mice (P25–P60), either control or bearing a chronic lesion of the dopaminergic fibers in the striatum, were killed by decapitation under halothane anesthesia. Oblique parasagittal slices (380 μ m thick) were cut with an angle of $10 \pm 2^\circ$ to obtain the BGS as previously described (Beurrier et al., 2006) (Fig. 1A1,B1). For the slicing procedure, the ice-cold oxygenated solution contained the following (in mM): 110 choline, 2.5 KCl, 1.25 NaH₂PO₄, 7 MgCl₂, 0.5 CaCl₂, 25 NaHCO₃, 7 glucose. To test for a possible role of choline, slices were also cut in a sucrose solution containing the following (in mM): 85 NaCl, 2.5 KCl, 1 NaH₂PO₄, 4 MgCl₂, 1 CaCl₂, 25 NaHCO₃, 25 glucose, 75 sucrose ($n = 4$). During the recovery period, BGSs were placed at room temperature (RT) with standard artificial CSF (ACSF) saturated with 95% O₂/5% CO₂ and containing the following (in mM): 126 NaCl, 3.5 KCl, 1.2 NaH₂PO₄, 1.3 MgCl₂, 2 CaCl₂, 25 NaHCO₃, 11 glucose. To isolate the striatum from its surrounding structures (cortex, thalamus, pallidum), we performed a knife cut along its borders under a dissecting microscope before the recording session (Fig. 1A2,B2). These slices were prepared to study the direct effect of bath-applied drugs on the striatal network.

Electrophysiology: solutions, data acquisition, and analysis. All recordings were made at 32°C. Cells were visualized with infrared-differential interference optics (Axioskop2; Zeiss). For whole-cell voltage-clamp recordings of postsynaptic GABA_A currents, the pipette (6–10 M Ω) contained the following (in mM): 120 Cs-gluconate, 13 CsCl, 1 CaCl₂, 10 HEPES, 10 EGTA, pH 7.2–7.4 (275–285 mOsm), or 110 CsCl, 30 K-gluconate, 0.1 CaCl₂, 10 HEPES, 1.1 EGTA, 4 MgATP, and 0.3 NaGTP. We used the CsGlu solution to measure spontaneous GABA_A currents at the reversal potential for glutamatergic (+10 mV) events (Cossart et al.,

2000) and the CsCl solution to measure the miniature GABA_A currents at $V_H = -60$ mV (in the continuous presence of $1 \mu\text{M}$ TTX plus $10 \mu\text{M}$ CNQX plus $40 \mu\text{M}$ APV). For current-clamp recordings, patch electrodes contained the following (in mM): 128.5 K-gluconate, 11.5 KCl, 1 CaCl₂, 10 EGTA, 10 HEPES, 2.5 MgATP, and 0.3 NaGTP, pH 7.32, 280 mOsm or the following (in mM): 125 KMeSO₄, 15 KCl, 5 NaCl, 10 HEPES, 2.5 Mg-ATP, 0.3 Na-GTP. The CsGlu, CsCl, and KGlu pipette solutions gave a reversal potential for chloride close to -58 , -5 , and -63 mV at 35°C , respectively. Biocytin (Sigma-Aldrich; 5 mg/ml) was added in all pipette solutions and osmolarity corrected when necessary. We performed patch-clamp recordings in whole-cell or cell-attached configuration using the Digidata 1344A interface, the Multiclamp 700A amplifier, and pClamp8 software (Molecular Devices). Spontaneous and miniature GABA_A receptor-mediated PSCs (sPSCs and mPSCs) were recorded at a holding potential of $+10$ and -60 mV, respectively. Currents were stored on pClamp8 (Molecular Devices) and analyzed off-line with Mini Analysis program (Synaptosoft 6.0), Clampfit 9.2, Origin 5.0, and Autosignal 1.7 to determine the frequency and amplitude of GABAergic synaptic events. All detected currents were then visually inspected to reject artifactual events. To generate the averaged GABA_A mPSCs, multiple overlapping events were first discarded, and the remaining events were aligned on their rising phase. Only MSNs that exhibited a stable pattern of GABA_A mPSCs during 20–30 min were taken into account. The histogram and cumulative distributions were constructed using GABA_A mPSCs recorded over 3 min. In the sPSC recordings, we defined as “giant” any sPSC with an amplitude >200 pA and as “burst” a minimum of five sPSCs associated with a baseline elevation. More than five giant events and three bursts were required during the 3 min analysis for the pattern to be deemed “oscillatory.”

For cell-attached recordings of single GABA_A channels, the pipette (4–5 M Ω) contained the following (in mM): 120 NaCl, 20 TEA-Cl (tetraethylammonium chloride), 5 KCl, 5 4-aminopyridine, 0.1 CaCl₂, 10 MgCl₂, 10 glucose, 10 HEPES-NaOH buffered to pH 7.2–7.3, osmolality of 300–320 mosmol. GABA ($5 \mu\text{M}$) was included in the above pipette saline together with isoguvacine ($5 \mu\text{M}$) and CsCl ($3 \mu\text{M}$) to optimize channel openings (because of the negative charge of GABA, positive currents may repulse GABA far from the membrane; under these conditions, isoguvacine may thus replace it). For single NMDA channels, pipettes were filled with nominally magnesium-free ACSF containing the following (in mM): 140 NaCl, 3.5 KCl, 1.8 CaCl₂, 10 HEPES, buffered to pH 7.43, osmolality of 300–320 mosmol. NMDA ($10 \mu\text{M}$) and glycine ($10 \mu\text{M}$) were included in the above saline to optimize channel openings and strychnine ($1 \mu\text{M}$) to block glycinergic receptors. For cell-attached recordings of neuronal activity, pipettes (4–5 M Ω) contained 150 mM NaCl. To identify the morphology of neurons recorded in cell-attached configuration, we repatched them with a conventional whole-cell electrode containing biocytin (see above). The single-channel currents were filtered at 1 kHz (GABA_A channels) or 3 kHz (NMDA channels) and digitized at 10 kHz. Multilevel and short (<2 ms) openings were discarded during analysis. I – V relationships were performed by measuring amplitude of unitary GABA and NMDA currents evoked by steps from -120 to $+40$ mV. Histograms of cursor-measured amplitudes allowed determination of the mean unitary current amplitude at each voltage tested. Series resistance (R_s), membrane capacitance (C_m), and input resistance (R_{input}) were determined by on-line fitting analysis of the transient currents in response to a $-5/10$ mV pulse. Criteria for considering a recording included $R_{\text{input}} > 100$ M Ω , $R_s < 25$ M Ω , with $\Delta R_s < 30\%$ change. Average values are presented as means \pm SEM and statistical comparisons were performed with the Student's t test (SigmaStat 3.1, Origin 5.0) or Mann–Whitney rank sum test (SigmaStat 3.1). The level of significance was set as $p < 0.05$.

We performed extracellular unit recording of striatal neurons with either conventional extracellular tungsten electrodes or with the multi-electrode array (MEA) technology (Heuschkel et al., 2002; Steidl et al., 2006). The MEA setup (Multi Channel Systems) is composed of a 60 channel amplifier head stage connected to a 60 channel A/D card. The slice is gently positioned on the array of 60 platinum electrodes (spaced by $100 \mu\text{m}$) used as recording electrodes (Ayanda Biosystems). Record-

ings were acquired and analyzed with the MC Rack software commercially available from Multi Channel Systems.

Measurements of V_{rest} , E_{GABA_A} , $V_{\text{threshold}}$. To determine the action of GABA in a given neuron (depolarizing or hyperpolarizing), one must measure the reversal potential of the GABA_A-mediated current (E_{GABA_A}) and the resting membrane potential (V_{rest}). However, conventional whole-cell recordings introduce a number of errors in these measures. We therefore estimated the value of V_{rest} from cell-attached recordings of the single-channel NMDA current (i_{NMDA}), which is known to reverse at a membrane potential (V_m) close to 0 mV (Nowak et al., 1984) (see Discussion). We plotted the relationship between i_{NMDA} and the extracellular potential applied to the patch of membrane (V_p) from experimental data (see Fig. 5A). This curve [$i_{\text{NMDA}} = f(V_p)$] gives the value of V_p when $i_{\text{NMDA}} = 0$ pA. At this value of V_p , single-channel NMDA current is null because $V_m = V_p - V_{\text{rest}} = 0$ mV. This allows estimation of V_{rest} ($V_{\text{rest}} = V_p$). To estimate (E_{GABA_A}), we plotted the relationship between the single-channel GABA_A current (i_{GABA_A}) and V_p . This curve [$i_{\text{GABA}_A} = f(V_p)$] gives the value of V_p when $i_{\text{GABA}_A} = 0$ pA (see Fig. 5B), because by definition when i_{GABA_A} is null, $V_m = E_{\text{GABA}_A}$. Therefore, when $i_{\text{GABA}_A} = 0$ pA, $V_m = V_p - V_{\text{rest}} = E_{\text{GABA}_A}$ (i.e., $E_{\text{GABA}_A} - V_{\text{rest}} = -V_p$). By definition, $E_{\text{GABA}_A} - V_{\text{rest}} = \text{DF}_{\text{GABA}_A}$, the driving force of chloride ions through the GABA_A channel (Tyzio et al., 2003). Therefore, when $i_{\text{GABA}_A} = 0$ pA, $\text{DF}_{\text{GABA}_A} = -V_p$. Knowing V_{rest} and $\text{DF}_{\text{GABA}_A}$, it is easy to calculate $E_{\text{GABA}_A} = \text{DF}_{\text{GABA}_A} + V_{\text{rest}}$. In addition, the slopes of the $i_{\text{NMDA}} - V_p$ and $i_{\text{GABA}_A} - V_p$ relationships provide an estimate of the conductance of NMDA and GABA_A channels, respectively. The threshold potential for Na⁺ spikes ($V_{\text{threshold}}$) was estimated in whole-cell current-clamp recordings by applying successive depolarizing steps [duration, 250 or 950 ms (Centonze et al., 2003)] or by evoking spikes by cortical stimulation, both from the value of V_{rest} calculated above.

Identification of recorded striatal neurons. We identified MSNs during recording based on their typical rectification during hyperpolarizing steps and their firing delay in response to depolarizing steps (see Fig. 5C). They had a round dendritic field with extremely spiny dendrites and axons that extended outside the striatum toward the globus pallidus (Fig. 1A3,B3). Cholinergic interneurons were readily identified in the slice by their large somata and thick primary dendrites. Negative-current pulses produced an initial hyperpolarization followed by a depolarizing sag in the membrane potential. Depolarizing pulses resulted in nonadapting, regular spiking. Examination of biocytin-filled neurons confirmed the above morphological criteria (see Fig. 6B). FS interneurons discharged in trains of narrow action potentials. Epochs of firing were interspersed with periods of silence during depolarizing steps just above threshold. Their aspiny dendrites branched modestly (see Fig. 7A). In addition to fast spikes, LTS interneurons also displayed low-threshold spikes when depolarized from potentials near -70 mV or after cessation of hyperpolarized pulses (see Fig. 7B). They had a high input resistance compared with the other neuronal types (~ 600 M Ω). Their dendrites radiated a long distance and were infrequently branched (Kawaguchi, 1993; Tepper and Bolam, 2004).

Drugs. Drugs were prepared as concentrated stock solutions and diluted in ACSF for bath application: bicuculline, a GABA_A receptor antagonist; carbachol, a cholinergic agonist; muscarine, a muscarinic cholinergic agonist; nicotine, a nicotinic cholinergic agonist; mecamylamine, a nicotinic antagonist; scopolamine, a muscarinic antagonist; D-APV, a NMDA receptor antagonist; 6-cyano-7-nitroquinoxaline 2,3-dione (CNQX), an AMPA/kainate receptor antagonist; tetrodotoxin (TTX), a Na⁺ channel blocker; $R(+)-7$ -chloro-8-hydroxy-3-methyl-1-phenyl-2,3,4,5-tetrahydro-1H-3-benzazepine hydrochloride (SCH23390), a D₁-like receptor antagonist; and sulpiride, a D₂ receptor antagonist. All drugs were purchased from Sigma-Aldrich.

Immunocytochemistry. To visualize the lesion of dopaminergic axons in the striatum, we performed immunocytochemistry of TH in the recorded slices, or those just medial or lateral to those recorded. After 12 h in paraformaldehyde (3%) at 4°C , the sections were rinsed in PBS and pretreated with 30% H₂O₂ (30 min) and blocked by 2% normal goat serum (NGS) in PBS containing 0.3% Triton X-100 for 30 min, and then incubated for 12 h with anti-TH polyclonal antibody (Pel-Freez) at a dilution of 1:1000. After rinsing with PBS, they were incubated for 1.5 h

with anti-mouse IgG secondary antibody (Tebu) at a dilution of 1:300 in PBS plus 2% normal goat serum. Sections were washed with PBS and incubated for 1.5 h in ABC complex at a dilution of 1:500 (Euromedex). They were rinsed and incubated for ~10 min in 3,3'-diaminobenzidine (DAB) (0.7 mg/ml) with peroxide (0.2 mg/ml) (SigmaFast), rinsed, mounted in Crystal/Mount (Electron Microscopy Sciences), coverslipped, and examined with a conventional microscope. Electrophysiological data were taken into account only when a severe loss (>90%) of tyrosine hydroxylase immunoreactivity was present in the dorsomedial striatum in which recordings were performed (Fig. 1B1,B2). To visualize the recorded cells in the striatum and identify them, we revealed the biocytin injected during whole-cell recordings. After 12 h in paraformaldehyde (3%) at 4°C, the sections were rinsed in PBS, left 12 h in 20% sucrose in phosphate buffer (PB), and left at -80°C for at least 2 h. They were thawed at room temperature, rinsed in PB, and incubated 30 min in 1% H₂O₂ in PB. Sections were washed with PB and KPBS and incubated for 12 h in ABC complex at a dilution of 1:100 in KPBS plus 0.3% Triton (Abcys). They were rinsed in KPBS and incubated for ~10 min in DAB (0.7 mg/ml) with peroxide (0.2 mg/ml) (SigmaFast), rinsed, mounted in Crystal/Mount (Electron Microscopy Sciences), coverslipped, and examined. Dendritic and axonal arbors were reconstructed for morphological analysis using the NeuroLucida system (MicroBrightField).

To identify the D₁ phenotype of the MSNs recorded, D₁R was detected by immunohistochemistry using a monoclonal antibody raised in rat against a 97 aa sequence corresponding to the C terminus of the human D₁R (Sigma-Aldrich) (Levey et al., 1993; Guigoni et al., 2007). Slices were cryoprotected in PBS with 25% saccharose, freeze-thawed in isopentane, and rinsed in PBS. Slices were then incubated in 4% NGS for 30 min and then in D₁R antibody (1:1000) supplemented with 1% NGS overnight at RT. After thorough rinsing, slices were incubated for 90 min at RT in Alexa 568 goat anti-rat (1:200 in PBS; Invitrogen) with streptavidin coupled with DTAF (dichlorotriazinylamino-fluorescein) (1:200; Fluor-Probes; Interchim) to detect biocytin injected in the recorded neurons. After thorough rinsing, slices were again incubated in D₁R antibody for 60 min, rinsed again, and incubated with secondary antibody for 60 min. This step was repeated once more. After thorough rinsing, slices were mounted in Vectashield (Vector Laboratories/Biovalley), coverslipped, and examined with a confocal microscope (Zeiss LSM 510).

Results

Spontaneous GABA_A currents increase in amplitude and shift to oscillatory mode in DA-depleted MSNs

We have recorded the activity of 97 control and 98 DA-depleted MSNs in slices of isolated striatum that have been disconnected from their glutamatergic afferent neurons (cortical and thalamic) and of 10 control and 18 DA-depleted MSNs in BGS. In whole-cell or cell-attached configuration (current-clamp mode), all the recorded MSNs were silent at resting membrane potential in both the control and DA-depleted states. The pattern of GABA_A sPSCs in identified MSNs ($n = 40$) was mainly tonic, with low-frequency (4.5 ± 0.4 Hz) and low-amplitude (34.1 ± 1.8 pA) events in isolated striatum (Fig. 2A). The overall mean current density of this tonic pattern was 459 ± 40 nA · ms (Fig. 2C, top). In 10 of the 40 MSNs, we also observed rare giant (>200 pA) currents (mean amplitude, 306 ± 8 pA; range, 200–650 pA; mean frequency, 0.14 ± 0.03 Hz) or rare bursts (mean intraburst frequency, 29.3 ± 1.1 Hz; mean intraburst amplitude, 51.3 ± 1.0 pA; $n = 3$ of 40) (Figs. 2A, middle and bottom traces; C, top; 3A, control). The results obtained in BGS were totally similar as those from isolated striatum (5.6 ± 1.0 Hz, $p = 0.31$; 30.0 ± 4.3 pA, $p = 0.44$).

After chronic DA depletion, a new pattern emerged, characterized by a higher current density (1311 ± 142 nA · ms) and the higher occurrence of giant GABA_A sPSCs such as (1) single sPSCs of higher amplitude (340 ± 6 pA; range, 240–1900 pA; $p < 0.01$) and frequency (0.29 ± 0.07 Hz; $p < 0.05$) compared with control

and (2) bursts of sPSCs, which recurred at regular intervals of 6.0 ± 0.8 s during periods varying from 6 to 1650 s (Fig. 2B1,C). The mean intraburst frequency of sPSCs (58.7 ± 1.3 Hz) and amplitude (95.9 ± 2.6 pA) both doubled compared with control ($p < 0.001$ for both) (Fig. 3A, DA-depleted). This new giant and oscillatory pattern was observed in 45% of the recorded MSNs ($n = 20$ of 45). In the remaining 55% MSNs ($n = 25$ of 45), the pattern of afferent GABA_A sPSCs was relatively unchanged by the DA lesion. The mean current density, frequency, and amplitude of sPSCs was not statistically different from control (496 ± 59 nA · ms, $p = 0.35$; 5.6 ± 0.6 Hz, $p = 0.11$; 35.3 ± 2.0 pA, $p = 0.67$; $n = 25$) (Fig. 2B2;C, top). The results obtained in DA-depleted BGS were similar as those recorded in isolated DA-depleted striatum with the presence of the oscillatory pattern of PSCs in 45% of MSNs (intraburst frequency, 73.3 ± 3.1 Hz, and intraburst amplitude, 111.4 ± 4.2 pA; giants amplitude, 270 ± 39 pA; $n = 8$ of 18) and of the regular pattern in the remaining 55%. In conclusion, spontaneous GABA_A sPSCs became strikingly oscillatory in ~50% of the MSNs in chronically DA-depleted striatum independently of the presence of corticostriatal neurons. We never observed such a pattern in control conditions.

The oscillatory pattern of GABA_A sPSCs did not depend on the internal pipette solution, holding membrane potential, or spontaneous glutamate synaptic activity. This pattern was observed with a recording solution with low internal chloride (CsGlu-filled electrodes) from $V_H = -75$ to $+10$ mV (Fig. 3B) or with high internal chloride (CsCl-filled electrode) (data not shown) and in the absence or presence of CNQX (10 – 30 μM) and APV (40 μM) (Fig. 3C). As expected, bicuculline (10 μM), an antagonist of GABA_A receptors, suppressed all sPSCs (Fig. 3C). To test whether the oscillatory pattern resulted from chronic or acute dopamine depletion, we acutely blocked dopaminergic transmission in control slices by simultaneously applying D₁R and D₂R antagonists (SCH23390, 10 μM; sulpiride, 10 μM). Acute blockade did not mimic chronic DA depletion. This treatment did not cause sPSCs to become oscillatory, nor did it significantly affect their frequency (from 6.6 ± 1.0 to 5.5 ± 1.5 Hz; $p = 0.91$) or amplitude (from 29.6 ± 1.6 to 24.8 ± 3.5 ; $p = 0.45$) (data not shown) ($n = 7$). This strongly suggested that the oscillatory pattern of GABA_A sPSCs resulted from the chronic, rather than acute, absence of dopaminergic terminals.

To understand whether giant currents had a postsynaptic or a presynaptic origin, we recorded miniature GABA_A currents. Their mean frequency and mean amplitude were not significantly different between control and DA-depleted MSNs that displayed the oscillatory pattern (frequency: 1.5 ± 0.2 Hz, $n = 15$, vs 1.8 ± 0.5 Hz, $n = 7$, $p = 0.5$; amplitude: 31.9 ± 1.5 pA, $n = 15$, vs 32.7 ± 2.8 , $n = 7$, $p = 0.8$), suggesting that the oscillatory pattern has a presynaptic origin (supplemental Fig. 1, available at www.jneurosci.org as supplemental material).

D₁-positive and D₁-negative MSNs generate the oscillatory pattern

Since MSNs are composed of D₂ striatopallidal and D₁ striatonigral subtypes, with a relatively selective distribution of D₁ and D₂ dopamine receptors that are not altered by chronic dopamine depletion (Nadjar et al., 2006), we reasoned that the two types of GABA_A sPSCs patterns recorded could correspond to these two types of MSNs. To test this hypothesis, we performed immunocytochemical labeling of intracellularly injected biocytin with D₁ dopamine receptor antibodies (see Materials and Methods). Of the 30 double-labeled MSNs recorded in DA-depleted striatum, 13 generated the oscillatory

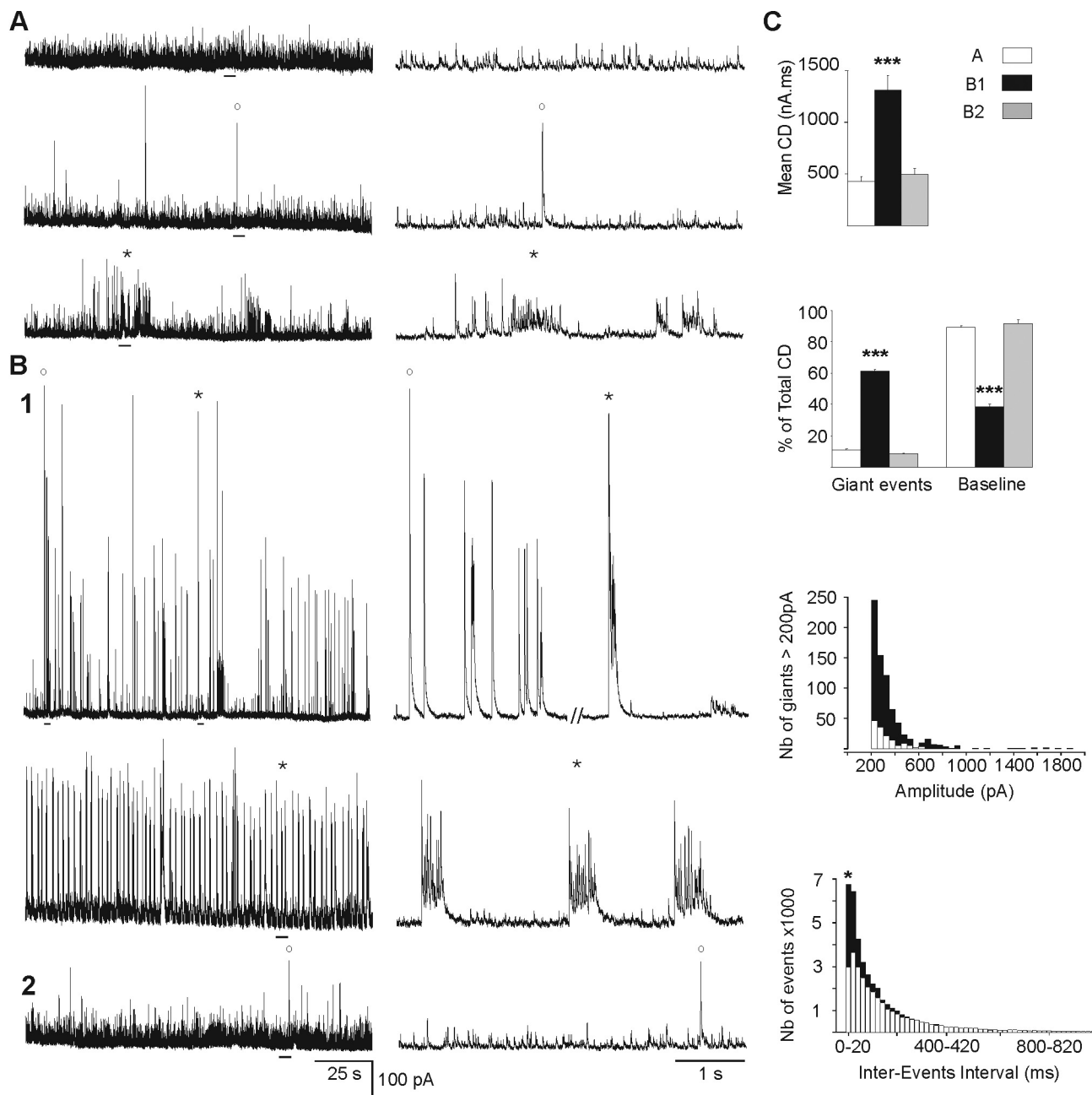


Figure 2. Spontaneous GABA_A currents recorded in MSNs before and after chronic DA depletion. Voltage-clamp recordings of GABA_A sPSCs with CsGlu-filled electrodes ($V_H = +10$ mV). **A**, Tonic pattern of GABA_A sPSCs in control isolated striatum (68% of MSNs; top traces) with the rare presence of single sPSCs (>200 pA) (23% of MSNs; middle traces) and bursts of sPSCs (*) (9% of MSNs; bottom traces). **B**, The two patterns of GABA_A sPSCs recorded from DA-depleted isolated striatum. **B1**, Oscillatory pattern observed in 45% of the MSNs and characterized by the frequent presence of giant events: single sPSCs (>200 pA) and bursts of sPSCs (*). **B2**, Tonic pattern in the remaining MSNs (55%). The calibration bars are the same for all recordings in **A** and **B**. **C** (from top to bottom), Quantification of the data from control MSNs as shown in **A** (white) and from DA-depleted MSNs as shown in **B1** (black) or **B2** (gray). The mean current density (CD) of GABA_A sPSCs increased threefold between **A** and **B1** or **B2** and **B1**. Giant events represented 11 and 8% of the total CD in **A** and **B2**, respectively, but 61% in **B1**. The baseline events (<200 pA) represented 89 and 92% of the total CD in **A** and **B2**, respectively, but 38% in **B1**. The distribution of single giant sPSCs >200 pA shows the increased number of these events and the presence of very large amplitude events (1000–1800 pA) in **B1** compared with **A**. Intervent intervals were shorter in **B1** than in **A** as most of the events were present in the interval 0–20 ms. Error bars indicate SEM. * $p < 0.05$; *** $p < 0.001$.

GABA_A pattern and 17 the tonic one. Among the 13 MSNs with the oscillatory pattern, 6 MSNs expressed D₁ dopamine receptors and 7 MSNs did not (Fig. 4). Among the 17 MSNs with a tonic GABA_A pattern, 4 MSNs expressed D₁ receptors and 13 MSNs did not. Therefore, both “D₁ positive” and “D₁ negative” MSNs can generate the oscillatory GABA_A pattern when dopamine deprived.

V_{rest} , E_{GABA_A} , and $V_{threshold}$ of MSNs are identical in control and DA-depleted striatum

Alterations of intrinsic parameters or the polarity of GABAergic synapses could also underlie the shift in the firing pattern of MSNs. Indeed, GABA signals in neuronal disorders have been reported to shift from inhibition to excitation (Cohen et al., 2002). To determine whether dopamine depletion leads to simi-

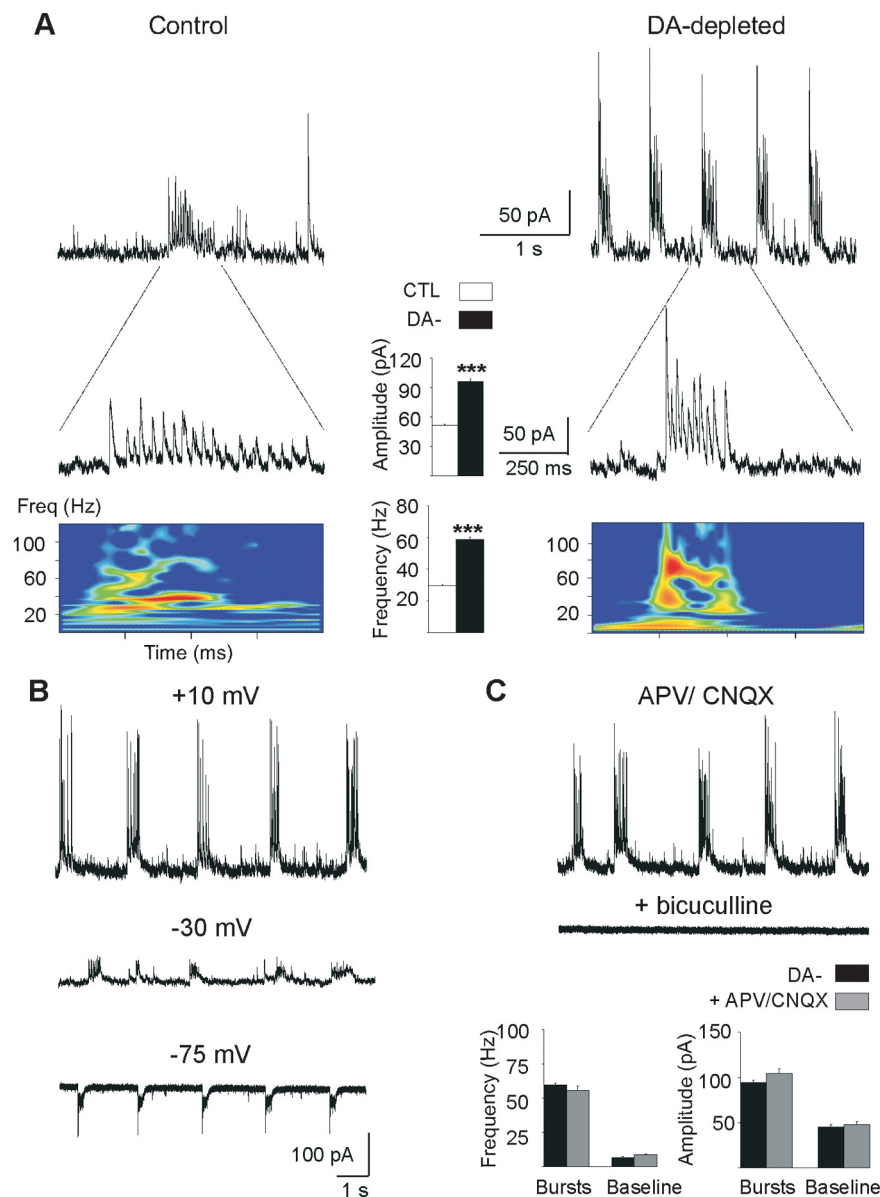


Figure 3. Burst characteristics. **A**, Whole-cell recordings ($V_H = +10$ mV) of rare bursts (**A**) and recurrent bursts (**B**) of GABA_A sPSCs in control (left) and DA-depleted (right) MSNs and corresponding power spectrum analysis of a single burst. Intraburst frequency of GABA_A sPSCs are visualized by time–frequency representations (bottom colored diagrams) that enables determining the implication of different frequency ranges within the burst. The field power is here coded in colors so that red corresponds to higher amplitudes. The calibrations are identical for the left and right traces. Histograms in the center, Mean intraburst amplitude and frequency of GABA_A sPSCs in control MSNs (□) and in DA-depleted MSNs with an oscillatory pattern (■). **B**, Recordings of recurrent bursts in a DA-depleted MSN at the indicated holding potentials (whole-cell configuration, internal CsGlu). **C**, Application of APV (40 μ M) plus CNQX (10 μ M) at $V_H = +10$ mV did not significantly affect the frequency and amplitude of bursts or baseline events (bottom histograms), whereas bicuculline at 20 μ M totally abolished them. Error bars indicate SEM. *** $p < 0.001$.

lar alterations, we performed single NMDA and GABA channel recordings to determine V_{rest} and E_{GABA_A} , respectively. We also measured the threshold for spike generation ($V_{threshold}$) (see Materials and Methods). Each tested neuron was successively patched in cell-attached configuration to record NMDA or GABA_A single-channel currents and then in whole-cell configuration to test the I – V relationship and label them with biocytin to confirm their identity as MSNs.

Current–voltage relationships of single NMDA channel currents from identified MSNs in control striatum yielded a mean resting membrane potential of $V_{rest} = -79.7 \pm 1.0$ mV ($n = 9$)

(mean NMDA conductance, 79 ± 3 pS; $n = 9$) (Fig. 5A). The extracellular Ca^{2+} concentration (1.8 mM) and the recording temperature (32°C) may explain this large conductance compared with the typical value obtained from cell-attached recordings in central neurons (50–60 pS) (Clark et al., 1997). Current–voltage relationships of single GABA_A channel currents recorded in identified MSNs yielded a mean driving force of $DF_{GABA_A} = 16.1 \pm 1.9$ mV ($n = 11$) (Fig. 5B), suggesting a mean reversal potential of GABA_A currents of $E_{GABA_A} = -63.6 \pm 2.9$ mV (conductance, 14.9 ± 1.1 pS; $n = 11$). The threshold potential for Na⁺ spikes in response to 250 ms depolarizing steps (Fig. 5C, control) was $V_{threshold} = -35.7 \pm 1.4$ mV ($n = 22$). The threshold of spikes evoked in response to cortical stimulation in control MSNs was $V_{threshold} = -38.3 \pm 0.6$ mV ($n = 7$) (Fig. 5C, control). $V_{threshold}$ obtained with these two methods were not statistically different ($p = 0.18$).

In DA-depleted striatum, the results obtained with the same methods were not statistically different from control: $V_{rest} = -80.1 \pm 1.0$ mV ($n = 7$; $p = 0.8$) (Fig. 5A, right), $DF_{GABA_A} = 17.1 \pm 1.6$ mV ($n = 10$; $p = 0.7$) (Fig. 5B, right), $E_{GABA_A} = -63.0 \pm 2.9$ mV ($n = 10$), and $V_{threshold} = -35.0 \pm 0.9$ mV ($n = 36$; $p = 0.6$) or -40.8 ± 1.0 mV for cortical stimulation evoked spikes ($n = 8$; $p = 0.06$) (Fig. 5C, right). Pressure-applied isoguvacine (100 μ M; 100 ms), a GABA_A receptor agonist, never excited control or DA-depleted MSNs recorded in cell-attached configuration ($n = 8$) (Fig. 5D). Therefore, in DA-depleted striatum GABA_A PSCs have the same effect on membrane potential of MSNs as in control striatum. Specifically, GABA depolarizes MSNs by 16–17 mV from V_{rest} (Fig. 5E), without evoking Na⁺ spikes, as the threshold potential for spikes was ~ 25 mV more depolarized than E_{GABA_A} .

GABA oscillations of DA-depleted MSNs are not mediated by cholinergic signaling

Several mechanisms could lead to the novel pattern of GABAergic oscillations observed, including changes in (1) activity of cholinergic interneurons, (2) presynaptic inhibition of GABA release by muscarinic receptors, (3) MSN–MSN recurrent collateral activity, or (4) activity of GABAergic interneurons, which would in turn generate GABA oscillations in MSNs. Interestingly, acetylcholine released by TANs excites GABA interneurons via nicotinic receptors (nAChRs) (Koós and Tepper, 2002), and in a primate Parkinson's disease model, TANs were said to shift to a bursting and oscillatory mode of activity (Raz et al., 1996). We performed the following pharmacological experiments in isolated striatum to avoid activation of structures afferent to striatum. Although nic-

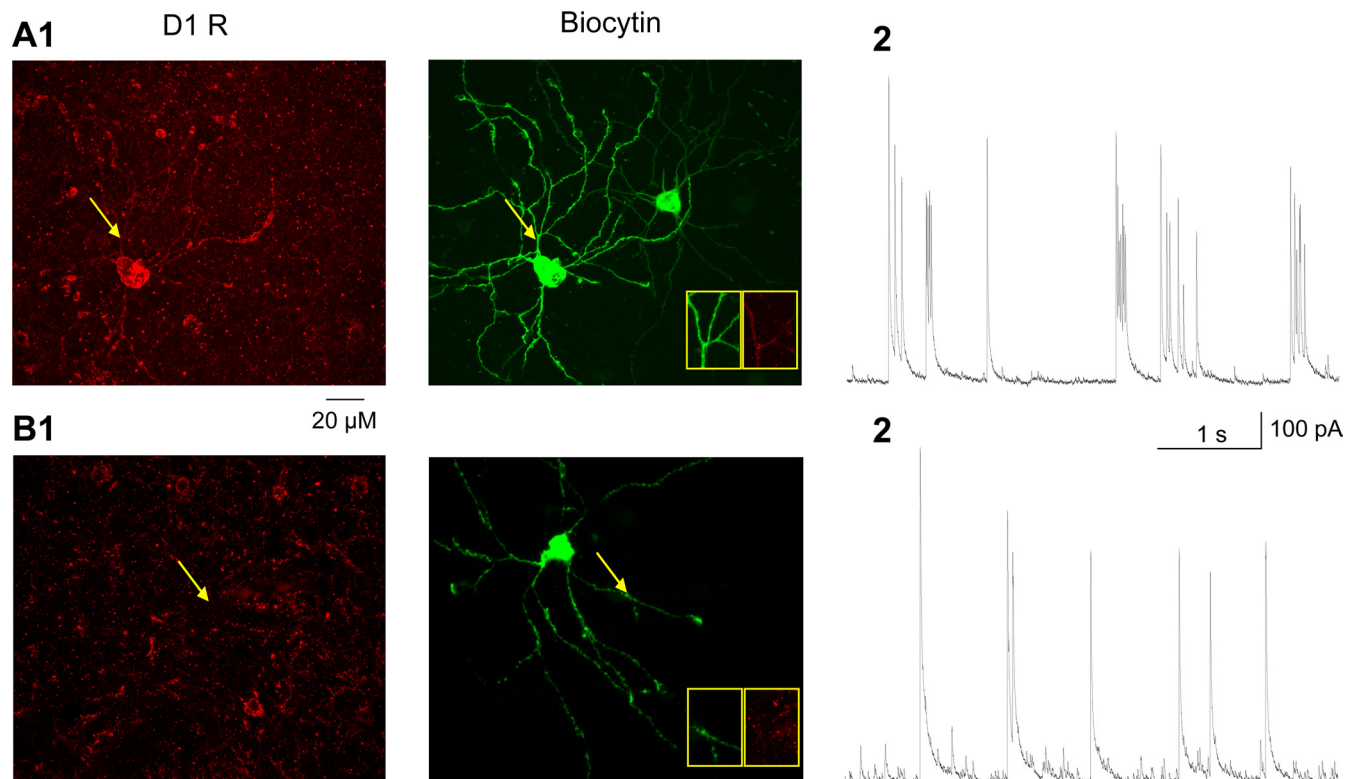


Figure 4. Oscillatory pattern recorded from MSNs positive (**A**) or negative (**B**) for D_1 dopamine receptor expression. Confocal microphotographs (z-projections) of DA-depleted slices, double labeled for D_1 receptor (red) and biocytin (green) (**A1**, **B1**). The boxes contain enlarged portions of dendritic arbors to show the presence (**A**) or the absence (**B**) of colabeling. In **A1**, the recorded MSN is on the left. The MSN on the right was indirectly filled with biocytin, likely because of gap junction connections with the recorded MSN. Both recorded neurons in **A** and **B** generated the oscillatory pattern of GABA_A sPSCs (**A2**, **B2**).

otine (10–30 μM) increased the mean current density of GABA_A sPSCs 13-fold (from 1655 ± 44 to $20,941 \pm 1052$ nA \cdot ms; $n = 7$; $p < 0.005$) (data not shown) in DA-depleted oscillating MSNs, the specific nicotinic antagonist mecamylamine (3–10 μM) altered neither their mean current density (from 2508 ± 862 to 1975 ± 985 nA \cdot ms; $n = 6$; $p = 0.13$) nor their oscillatory pattern (Fig. 6A). Alternately, acetylcholine released by TANs could affect GABA interneurons via muscarinic receptors (mAChRs). Muscarine (10 μM) did not significantly affect the current density of oscillatory GABA_A sPSCs ($n = 6$) (data not shown), and scopolamine (10 μM), a broad spectrum muscarinic antagonist, also did not affect their mean current density (from 1894 ± 300 to 1497 ± 400 nA \cdot ms; $n = 5$; $p = 0.21$) or their oscillatory pattern (Fig. 6A).

To further investigate a presynaptic modulation by muscarinic receptors of GABA release (Koós and Tepper, 2002), we determined the effects of carbachol on miniature GABA_A sPSCs. Carbachol (30 μM) significantly decreased this frequency by 33% in control striatum (from 1.5 ± 0.2 to 1.0 ± 0.1 Hz; $p < 0.01$; $n = 9$ cells), an effect that was totally reversed by scopolamine (10 μM) (from 1.0 ± 0.1 to 1.9 ± 0.2 Hz; $n = 9$ cells) (supplemental Fig. 1A, available at www.jneurosci.org as supplemental material). In DA-depleted striatum, carbachol decreased the frequency of miniature GABA_A events by 18% (from 2.2 ± 0.5 to 1.8 ± 0.5 Hz; $p < 0.05$; $n = 9$ cells), an effect that was completely reversed by scopolamine (from 1.8 ± 0.5 to 2.2 ± 0.6 Hz; $n = 9$ cells). The effects of carbachol on miniature GABA_A currents was not statistically different between control and DA-depleted striatum ($p = 0.12$) (supplemental Fig. 1B, available at www.jneurosci.org as supplemental material).

Finally, cell-attached recordings of identified TANs confirmed that DA-depletion did not affect their tonic pattern of activity recorded *in vitro* (mean control frequency, 2.7 ± 1.1 Hz; $n = 9$; mean DA-depleted frequency, 4.0 ± 1.4 Hz; $n = 8$; $p = 0.4$) nor their basic characteristics (Fig. 6B). All of the above results strongly suggest that the oscillatory pattern of GABA_A sPSCs is independent of TAN activity.

LTS GABA interneurons show bursting activity in DA-depleted slices

Because all MSNs recorded in cell-attached or whole-cell configuration were silent in both control and DA-depleted striatum (Fig. 5D) and the strength of MSN–MSN connections dramatically reduced in DA-depleted conditions (Taverna et al., 2008), the synchronization of GABA_A currents observed here likely resulted from a direct effect of chronic dopamine depletion on the activity of GABAergic interneurons. As these interneurons are rare and difficult to target with single-cell electrophysiological techniques, particularly in lesioned tissue, we first performed extracellular recordings with conventional extracellular electrodes or multiarray electrodes (see Materials and Methods) to test for the presence of oscillatory activities under control or lesioned conditions. In control BGS ($n = 3$ slices) and control isolated striatum ($n = 12$ slices), we never recorded oscillatory activities. Neurons were either silent or showed single-spike activity. In contrast, in DA-depleted BGS ($n = 2$) and isolated striatum ($n = 11$), oscillatory activity was observed together with single-spike activity (data not shown).

Cell-attached recordings combined with subsequent whole-cell recording of spike responses to intracellular current steps and

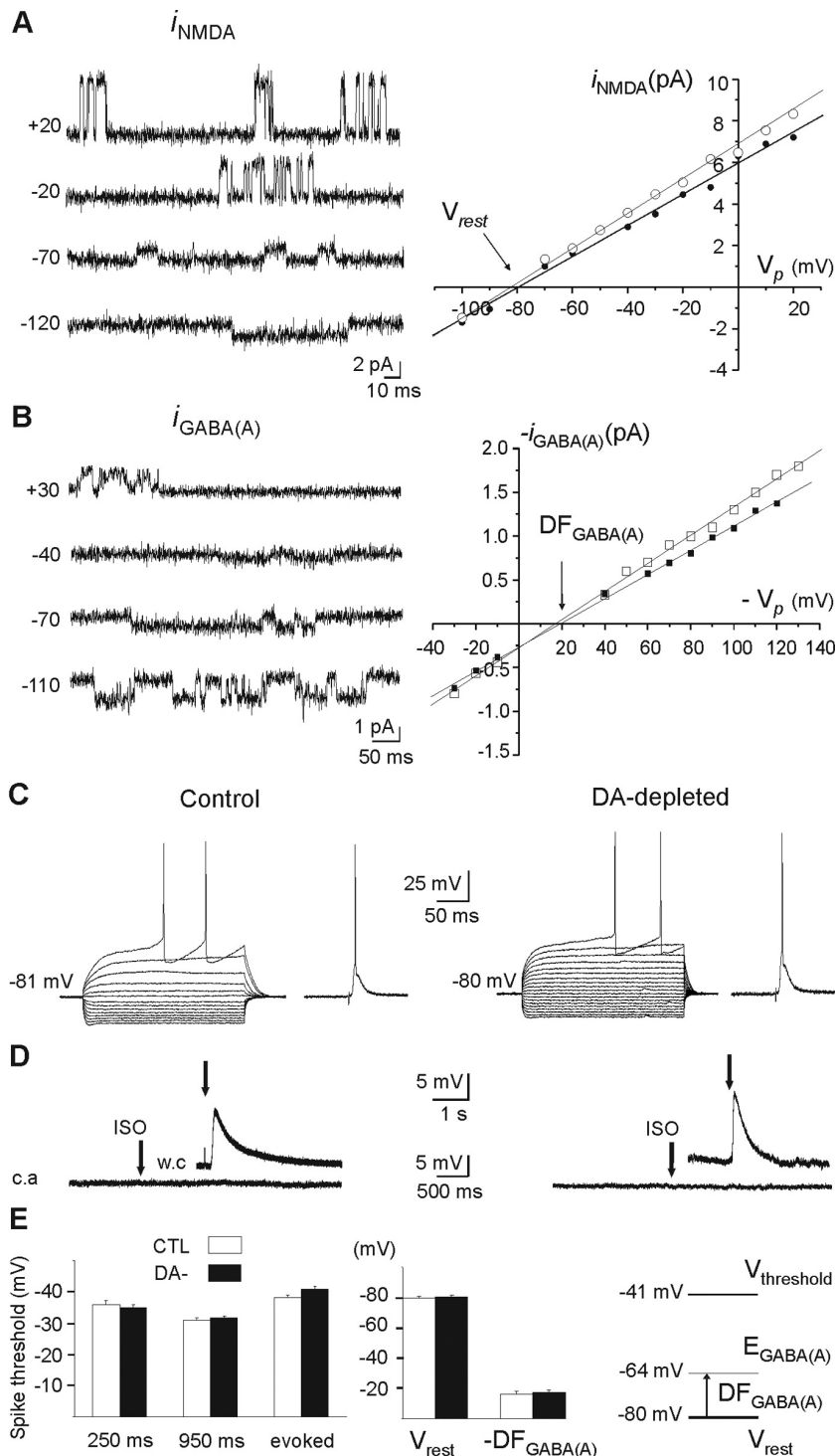


Figure 5. V_{rest} , $E_{GABA(A)}$, and $V_{threshold}$ in MSNs of control and DA-depleted striatum. **A**, Cell-attached recordings of unitary NMDA currents at the indicated holding potentials (in millivolts) from a DA-depleted MSN (left) and i_{NMDA} - V relationship in control (○) and DA-depleted (●) MSNs (right). **B**, Cell-attached recordings of unitary GABA_A currents at the indicated holding potentials (in millivolts) from a DA-depleted MSN (left) and $i_{GABA(A)}$ - V relationship in control (○) and DA-depleted (●) MSNs (right). The illustrated traces and corresponding I - V curves for NMDA and GABA currents are from the same cells. **C**, Whole-cell current-clamp recordings of the responses of control (left) and DA-depleted (right) MSNs to intracellular hyperpolarizing and depolarizing steps and to cortical stimulation. **D**, Absence of excitatory responses of cell-attached (c.a.) recorded MSNs to local pressure application of isoguvacine (100 μ M), a GABA_A receptor agonist, in control (left) and DA-depleted (right) state. The insets show the depolarizing effect of isoguvacine (100 μ M) after rupture of the membrane [whole-cell recording (w.c.)] to check the efficacy of pressure application. **E**, Spike threshold was not significantly different in control and DA-depleted MSNs when tested in response to 250 or 950 ms intracellular currents pulses or evoked by cortical stimulation. Resting membrane potential (V_{rest}), driving force for chloride ions ($DF_{GABA(A)}$) or reversal potential for GABA_A current, and threshold potential for spikes ($V_{threshold}$) were not significantly different in control and DA-depleted MSNs. Error bars indicate SEM. See Results for additional explanations.

post hoc morphological examination of the recorded neurons showed that FS (Fig. 7A, left) and LTS (Fig. 7B, left) interneurons were silent or tonically active in control striatum. FS mean frequency of activity was 10.1 ± 0.2 Hz ($n = 2$ of 5) and LTS mean frequency was 8.8 ± 1.1 Hz with rare trains at ~ 20 Hz ($n = 3$ of 5). In lesioned conditions, FS interneurons still discharged in single-spike mode (7.4 ± 2.5 Hz; $n = 6$ of 18) or stayed silent (Fig. 7, compare B3, B4, with A3, A4). In contrast, some LTS interneurons shifted to an oscillatory activity consisting of long bursts of spikes at a mean frequency of 71 ± 30 Hz separated by silent periods of 3.9 ± 1.6 s ($n = 3$ of 5). This LTS bursting activity was insensitive to the presence of blockers of glutamatergic transmission (Fig. 7B4), suggesting that it is not generated by corticostriatal activity. The remaining LTS displayed a tonic activity at 9.7 ± 1.7 Hz ($n = 2$ of 5). Interestingly, the intraburst frequency of spikes generated by LTS interneurons in DA-depleted condition was close to the intraburst frequency of GABA_A currents recorded in DA-depleted MSNs (see results above).

Discussion

Our results show that chronic dopamine depletion profoundly alters the pattern of GABA_A activity, shifting the currents in one-half of the MSN population from a continuous tonic pattern of sPSCs to an oscillatory pattern consisting of giant single sPSCs, and/or bursts of sPSCs at a gamma frequency (~ 60 Hz). Using, for the first time, single-channel recordings of NMDA and GABA receptors in the striatum, we show that these alterations are not associated with shifts of the reversal potential for GABA or the resting membrane potential, suggesting that they are not attributable to excitatory actions of GABA. The threshold for spike generation is also unaltered by chronic dopamine depletion and cholinergic signals are not involved. We propose that the fundamental effect of the chronic removal of dopaminergic control on GABAergic circuits of the striatum is the shift of activity of GABAergic LTS interneurons from single-spike to bursting pattern and the increase in efficacy of GABAergic synaptic transmission. This leads in turn to the generation of repetitive giant bursts of GABA currents by one-half of the MSN population.

In both sagittal striatal slices from control mice (the present experiment) and coronal slices from control rats (Centonze et al., 2004; Cummings et al., 2008), MSNs generate a tonic pattern of low amplitude

GABA_A currents (5–30 pA) at low frequency (~2.5–4 Hz). DA depletion shifted this pattern to an oscillatory one in D₁-positive as well as D₁-negative MSNs, suggesting that the effect of DA depletion on the pattern of GABA_A currents did not target a particular subpopulation of MSNs. The 55% of the MSNs that generated the tonic GABA_A pattern rather than the oscillatory one may be explained by their low degree of connectivity to GABA interneurons in the slice, or to a true difference in GABAergic innervation between the two MSNs groups.

What is the origin of the shift to the oscillatory pattern? Cholinergic interneurons, the TANs, were good candidates, as they are supposed to oscillate in the chronic absence of dopamine (Raz et al., 1996). However, in our experimental conditions, nicotinic and muscarinic blockers did not affect the oscillatory pattern, and identified TANs displayed the same tonic pattern of activity in the presence or absence of dopaminergic innervation. In simultaneous whole-cell recording of pairs of FS interneurons and MSNs, acetylcholine attenuates GABAergic inhibition of MSNs through activation of presynaptic muscarinic receptors located on GABA axon terminals (Marchi et al., 1990; Koós and Tepper, 2002). We showed that dopamine depletion of the striatum does not affect this process, suggesting that chronic alterations of presynaptic inhibition of GABA release by muscarinic receptors is also unlikely to be responsible for the generation of oscillatory GABA sPSCs. Concerning presynaptic control of GABA release by dopamine receptors, recordings of spontaneous GABA_A currents from D₂ receptor knock-out mice revealed a loss of the inhibitory effect of the D₂ agonist quinpirole (Centonze et al., 2004).

Therefore, dopamine deprivation may produce a dual action: alteration of the basic activity pattern of a subpopulation of GABA interneurons, and decrease of presynaptic inhibition of GABA release leading to repetitive giant GABA_A currents. Approximately 4–27 FS interneurons project to each MSN (Koós and Tepper, 1999), and each FS cell establishes a mean of six release sites per MSN (up to 18) that are often organized in clusters of synaptic contacts on the soma or proximal dendrites (Kita et al., 1990). This distribution and the proximity to the cell body enable an efficient inhibitory control of MSNs. In contrast, MSN–MSN recurrent synapses are on distal dendrites with only a small number of release sites (average of three) (Wilson and Groves, 1980). These may thus be less prone to generation of giant sPSCs. Despite the relatively high degree of convergence (each MSN receives ~500 synapses from other MSNs) (Czubayko and Plenz, 2002; Guzmán et al., 2003; Koós et al., 2004), this recurrent system is unlikely to mediate the generation of giant GABAergic currents, because MSNs were silent in BGS and isolated striatum and their strength mostly de-

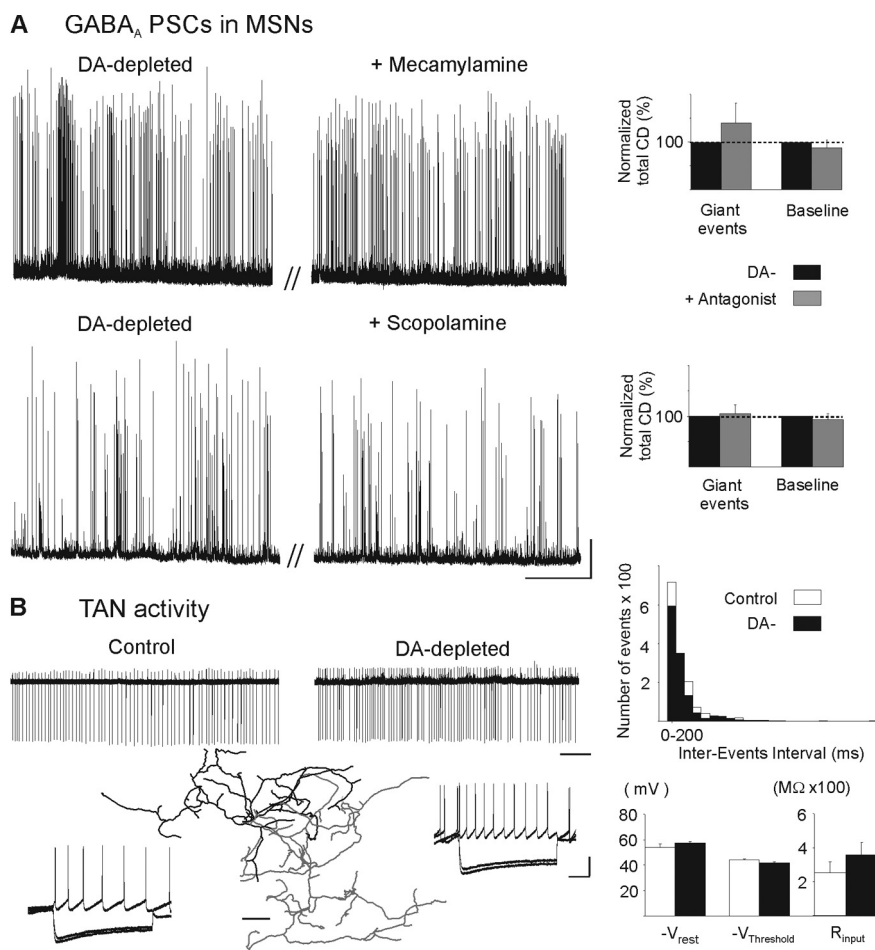


Figure 6. Effect of cholinergic antagonists on the oscillatory pattern of GABA_A sPSCs and TAN activity in DA-depleted state. **A**, Lack of effect of bath application of mecamylamine (5 μ M) (top traces) or scopolamine (10 μ M) (bottom traces) on the oscillatory pattern of GABA_A sPSCs recorded in MSNs from DA-depleted isolated striatum. These nicotinic and muscarinic receptor antagonists did not affect current density (CD) of giant or baseline events of the oscillatory pattern (right diagrams). **B**, Current-clamp, cell-attached (top), and subsequent whole-cell (bottom) recordings from the same TANs in control (left) or in DA-depleted BGS (right). Current steps were applied from V_{rest} = -57 mV in control and -59 mV in DA-depleted TANs to V_m = -90 , -85 , and -40 mV. Notice the characteristic sag in response to hyperpolarizing current steps. NeuroLucida reconstruction of a biocytin-filled TAN with its dendritic tree in black and its collateralized axon in gray. Scale bar, 50 μ m. DA depletion did not affect TANs spontaneous pattern of activity (see the distribution of interevents intervals) nor their mean values of V_{rest} (-54.0 ± 2.7 vs -57.2 ± 1.2 mV; $n = 7$ and 11 ; $p = 0.4$), $V_{threshold}$ (-44.2 ± 0.3 vs -41.7 ± 0.9 mV; $n = 7$ and 11 ; $p = 0.1$) and input resistance (R_{input}) (255 ± 63 vs 357 ± 74 M Ω ; $p = 0.4$) (right diagrams). Calibration: **A**, 25 s, 100 pA; **B**, 5 s (top) and 200 ms, 25 mV (bottom steps). Error bars indicate SEM.

creased in the chronic absence of dopamine (Taverna et al., 2008). FS interneurons are also unlikely to mediate bursts of GABAergic currents because DA depletion did not affect their single-spike firing pattern. In contrast, we showed for the first time that identified LTS interneurons spontaneously discharge with a striking bursting pattern in the absence of dopamine, a type of activity not recorded under control conditions. Moreover, the intraburst frequency of LTS spikes was close to that of GABAergic currents recorded in MSNs.

Our single GABA and NMDA channel recordings (Tyzio et al., 2003) indicate for the first time a value for the reversal potential of GABA current ($E_{GABA} = -63.0 \pm 2.9$ mV) of DA-depleted MSNs. We also showed that the resting membrane potential ($V_{rest} = -80$ mV) and E_{GABA} of MSNs are not affected by dopamine depletion. All these values are based on the assumption that the NMDA current reverses at 0 mV in MSNs. Although an error of ~5 mV may exist (Tyzio et al., 2003), the comparison of V_{rest}

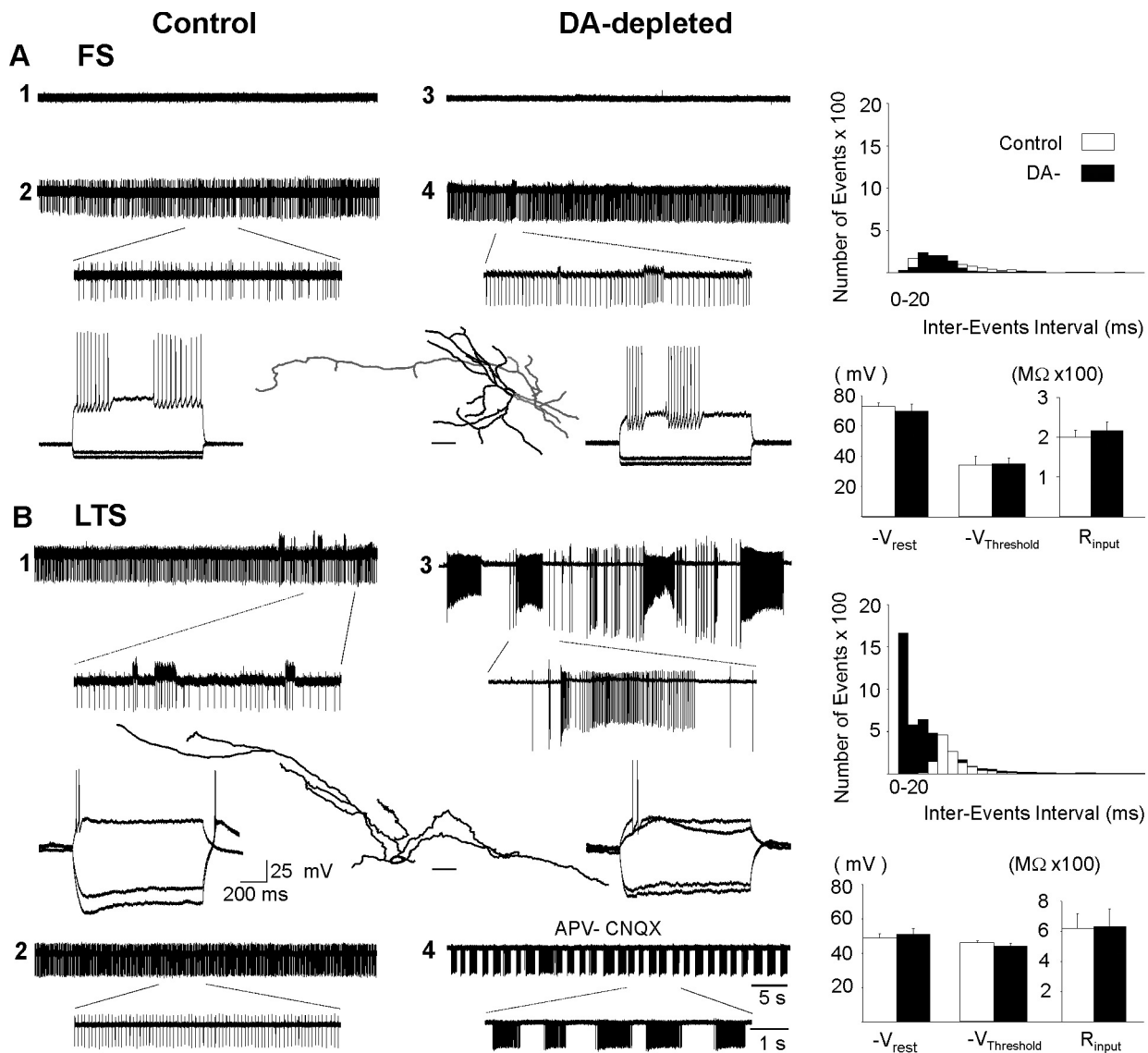


Figure 7. Spontaneous activity of GABAergic FS and LTS interneurons in control and DA-depleted striatum. **A**, Activity of FS interneurons recorded in cell-attached configuration in control (**1, 2**) and DA-depleted (**3, 4**) striatum. Sixty percent of FS were silent in control striatum (**1**) and 67% in DA-depleted one (**3**). The remaining FS displayed single-spike regular activity with rare trains of spikes (**4**). The bottom traces in **2** and **4** are expanded traces of the top ones as indicated. Note the typical FS firing in response to depolarizing steps (bottom traces) recorded in control from neuron 2 and in DA-depleted striatum from neuron 4. Current steps were applied from $V_{rest} = -74.8$ mV to $V_m = -82$, -78 , and -29 mV in control and from $V_{rest} = -78$ mV to -90 , -85 , and -37 mV in DA-depleted FS neurons. Neurolucida reconstruction of the biocytin-filled FS interneuron 2 show the aspiny dendrites (black) and the collateralized axon (gray). The right diagrams show that the interevent intervals distribution and the mean value of V_{rest} (-73.0 ± 2.3 vs -69.6 ± 5.0 mV; $n = 5$ and 6 ; $p = 0.6$), $V_{threshold}$ (-34.0 ± 5.8 vs -34.8 ± 3.7 mV; $n = 5$ and 7 ; $p = 0.9$), and input resistance (R_{input}) (199 ± 18 vs 217 ± 21 M Ω ; $n = 5$ and 7 ; $p = 0.6$) were unchanged by DA depletion. **B**, LTS interneurons switch from a tonic control activity to a bursting one in DA-depleted condition. Two examples of control (**1, 2**) and DA-depleted (**3, 4**) LTS activities are shown. LTS in **4** was recorded in the continuous presence of the glutamatergic antagonists APV (10 μ M) and CNQX (40 μ M). Note the typical rebound after hyperpolarizing steps giving rise to spikes and the low-threshold Ca^{2+} spike in response to depolarizing steps (bottom traces) recorded in control from neuron 1 and in DA-depleted striatum from neuron 3. Current steps were applied from $V_m = -70$ mV to $V_m = -130$, -115 , and -43 mV in control and from $V_m = -71$ mV to -120 , -115 , -55 , and -47 mV in DA-depleted LTS neurons. Neurolucida reconstruction of the biocytin-filled LTS interneuron 3 show the extended dendritic field and the aspiny dendrites (the axon was not visible). The right diagrams show that the interevent intervals distribution was shifted to the left. The mean values of V_{rest} (-48.7 ± 2.5 vs -51.0 ± 3.1 mV; $n = 5$ and 6 ; $p = 0.6$), $V_{threshold}$ (-46.5 ± 0.7 vs -42.4 ± 1.4 mV; $n = 5$ and 5 ; $p = 0.06$), and input resistance (R_{input}) (622 ± 97 vs 630 ± 118 M Ω ; $n = 5$ and 6 ; $p = 0.9$) were unchanged by DA depletion. Calibrations are identical for all cell-attached recordings (5 s for main traces and 1 s for enlarged ones) and for all whole-cell recordings (25 mV, 200 ms). Scale bar for neurons, 50 μ m. Error bars indicate SEM.

and E_{GABA} obtained with the same methods in control and DA-depleted MSNs confirms the validity of our conclusions. Another noninvasive method to determine V_{rest} consists in estimating the reversal potential for K^+ ions using cell-attached recordings with pipettes containing 145–155 mM K^+ ions. With the symmetric K^+ gradient, the K^+ current through the membrane patch reverses when the potential of the pipette is equal to the membrane potential (V_{rest}) (Verheugen et al., 1999). This measure is based on the approximation of the internal K^+ concentration. Interest-

ingly, both protocols (single NMDA current or equimolar K^+) gave similar results ($-80/-81$ mV) in control MSNs (Ade et al., 2008). These values are also close to those obtained with gramicidin perforated patch that leaves the internal chloride concentration intact (-81 and -64 ± 4 mV, respectively) (Bracci and Panzeri, 2006) [for more depolarized values in organotypic cultures, see also Gustafson et al. (2006)]. Our determination of spike threshold in control and DA-depleted MSNs in whole-cell recordings and K Glu electrodes is close to that previously identi-

fied under the same conditions [-36 mV (Taverna et al., 2007); -38 mV (Fino et al., 2007)]. Therefore, GABAergic synapses depolarize MSNs from V_{rest} (Misgeld et al., 1982; Koós and Tepper, 1999) but do not trigger action potentials and hence can exert inhibitory actions (Plenz and Aertsen, 1996). The membrane potential of MSNs *in vivo*, under urethane or sodium pentobarbital anesthesia, oscillates between down and up states, the latter being generated by glutamatergic afferents (Wilson and Kawaguchi, 1996; Mahon et al., 2001; Tseng et al., 2001). Spontaneous or evoked activation of GABA_A receptors depolarize the MSN membrane *in vivo* during the down state (Mercuri et al., 1991) and hyperpolarize it during the up state (Plenz and Kitai, 1998), suggesting that GABA exerts an inhibitory action on MSN activity.

We propose that the fundamental feature of the dopamine-deprived isolated striatum is a shift from a continuous tonic GABA pattern to one that oscillates between repetitive giant sPSCs and silent episodes. This results from alterations of the firing properties of a subpopulation of GABA interneurons that shifts from low-frequency tonic to high-frequency oscillatory activity. The shift in the GABA_A pattern may profoundly alter the response of one-half the MSNs to cortical inputs *in vivo*, thus destabilizing striatal function. During down states, GABA-induced depolarization decreases the impact of the hyperpolarization-activated inward rectifier K⁺ current that prevents MSNs from excitation-induced rapid firing (Surmeier and Kitai, 1993; Nicola et al., 2000). It will also drive the MSN membrane to a potential (-65 mV) at which its input resistance and time constant are close to maximal (Wilson, 2007), which may facilitate glutamatergic inputs and lead to the generation of action potentials (Bracci and Panzeri, 2006). Along the same lines, blockade of spontaneous and tonic GABA_A synaptic transmission decreased the cortically evoked excitation recorded from MSNs in the cell-attached configuration (Ade et al., 2008). In contrast, during up states that are more frequent in DA-depleted striatum [MSNs spend a longer time in up states in chronically 6-hydroxydopamine-lesioned rats (Murer et al., 2002)], giant GABAergic currents should efficiently and transiently inhibit cortical inputs, preventing information transfer and integration.

References

- Ade KK, Janssen MJ, Ortinski PI, Vicini S (2008) Differential tonic GABA conductances in striatal medium spiny neurons. *J Neurosci* 28:1185–1197.
- Bennett BD, Bolam JP (1994) Localisation of parvalbumin-immunoreactive structures in primate caudate-putamen. *J Comp Neurol* 347:340–356.
- Beurrier C, Ben-Ari Y, Hammond C (2006) Preservation of the direct and indirect pathways in an *in vitro* preparation of the mouse basal ganglia. *Neuroscience* 140:77–86.
- Bracci E, Panzeri S (2006) Excitatory GABAergic effects in striatal projection neurons. *J Neurophysiol* 95:1285–1290.
- Bracci E, Centonze D, Bernardi G, Calabresi P (2002) Dopamine excites fast-spiking interneurons in the striatum. *J Neurophysiol* 87:2190–2194.
- Calabresi P, Picconi B, Tozzi A, Di Filippo M (2007) Dopamine-mediated regulation of corticostriatal synaptic plasticity. *Trends Neurosci* 30:211–219.
- Centonze D, Bracci E, Pisani A, Gubellini P, Bernardi G, Calabresi P (2002) Activation of dopamine D1-like receptors excites LTS interneurons of the striatum. *Eur J Neurosci* 15:2049–2052.
- Centonze D, Grande C, Usiello A, Gubellini P, Erbs E, Martin AB, Pisani A, Tognazzi N, Bernardi G, Moratalla R, Borrelli E, Calabresi P (2003) Receptor subtypes involved in the presynaptic and postsynaptic actions of dopamine on striatal interneurons. *J Neurosci* 23:6245–6254.
- Centonze D, Gubellini P, Usiello A, Rossi S, Tschertner A, Bracci E, Erbs E, Tognazzi N, Bernardi G, Pisani A, Calabresi P, Borrelli E (2004) Differential contribution of dopamine D2S and D2L receptors in the modulation of glutamate and GABA transmission in the striatum. *Neuroscience* 129:157–166.
- Clark BA, Farrant M, Cull-Candy SG (1997) A direct comparison of the single-channel properties of synaptic and extrasynaptic NMDA receptors. *J Neurosci* 17:107–116.
- Cohen J, Navarro V, Clemenceau S, Baulac M, Miles R (2002) On the origin of interictal activity in human temporal lobe epilepsy *in vitro*. *Science* 298:1418–1421.
- Cossart R, Hirsch JC, Cannon RC, Dinoncourt C, Wheal HV, Ben-Ari Y, Esclapez M, Bernard C (2000) Distribution of spontaneous currents along the somato-dendritic axis of rat hippocampal CA1 pyramidal neurons. *Neuroscience* 99:593–603.
- Cummings DM, Yamazaki I, Cepeda C, Paul DL, Levine MS (2008) Neuronal coupling via connexin36 contributes to spontaneous synaptic currents of striatal medium-sized spiny neurons. *J Neurosci Res* 86:2147–2158.
- Czubayko U, Plenz D (2002) Fast synaptic transmission between striatal spiny projection neurons. *Proc Natl Acad Sci U S A* 99:15764–15769.
- Fino E, Glowinski J, Venance L (2007) Effects of acute dopamine depletion on the electrophysiological properties of striatal neurons. *Neurosci Res* 58:305–316.
- Guigoni C, Doudnikoff E, Li Q, Bloch B, Bezard E (2007) Altered D(1) dopamine receptor trafficking in parkinsonian and dyskinetic non-human primates. *Neurobiol Dis* 26:452–463.
- Gustafson N, Gireesh-Dharmaraj E, Czubayko U, Blackwell KT, Plenz D (2006) A comparative voltage and current-clamp analysis of feedback and feedforward synaptic transmission in the striatal microcircuit *in vitro*. *J Neurophysiol* 95:737–752.
- Guzmán JN, Hernández A, Galarraga E, Tapia D, Laville A, Vergara R, Aceves J, Bargas J (2003) Dopaminergic modulation of axon collaterals interconnecting spiny neurons of the rat striatum. *J Neurosci* 23:8931–8940.
- Heuschkel MO, Fejtl M, Raggenbass M, Bertrand D, Renaud P (2002) A three-dimensional multi-electrode array for multi-site stimulation and recording in acute brain slices. *J Neurosci Methods* 114:135–148.
- Iancu R, Mohapel P, Brundin P, Paul G (2005) Behavioral characterization of a unilateral 6-OHDA-lesion model of Parkinson's disease in mice. *Behav Brain Res* 162:1–10.
- Kawaguchi Y (1993) Physiological, morphological, and histochemical characterization of three classes of interneurons in rat neostriatum. *J Neurosci* 13:4908–4923.
- Kita H, Kosaka T, Heizmann CW (1990) Parvalbumin-immunoreactive neurons in the rat neostriatum: a light and electron microscopic study. *Brain Res* 536:1–15.
- Koós T, Tepper JM (1999) Inhibitory control of neostriatal projection neurons by GABAergic interneurons. *Nat Neurosci* 2:467–472.
- Koós T, Tepper JM (2002) Dual cholinergic control of fast-spiking interneurons in the neostriatum. *J Neurosci* 22:529–535.
- Koós T, Tepper JM, Wilson CJ (2004) Comparison of IPSCs evoked by spiny and fast-spiking neurons in the neostriatum. *J Neurosci* 24:7916–7922.
- Kubota Y, Kawaguchi Y (2000) Dependence of GABAergic synaptic areas on the interneuron type and target size. *J Neurosci* 20:375–386.
- Levey AI, Hersch SM, Rye DB, Sunahara RK, Niznik HB, Kitt CA, Price DL, Maggio R, Brann MR, Ciliax BJ (1993) Localization of D1 and D2 dopamine receptors in brain with subtype-specific antibodies. *Proc Natl Acad Sci U S A* 90:8861–8865.
- Mahon S, Deniau JM, Charpier S (2001) Relationship between EEG potentials and intracellular activity of striatal and cortico-striatal neurons: an *in vivo* study under different anesthetics. *Cereb Cortex* 11:360–373.
- Mallet N, Le Moine C, Charpier S, Gonon F (2005) Feedforward inhibition of projection neurons by fast-spiking GABA interneurons in the rat striatum *in vivo*. *J Neurosci* 25:3857–3869.
- Marchi M, Sanguineti P, Raiteri M (1990) Muscarinic receptors mediate direct inhibition of GABA release from rat striatal nerve terminals. *Neurosci Lett* 116:347–351.
- Mercuri NB, Calabresi P, Stefani A, Stratta F, Bernardi G (1991) GABA depolarizes neurons in the rat striatum: an *in vivo* study. *Synapse* 8:38–40.
- Misgeld U, Wagner A, Ohno T (1982) Depolarizing IPSPs and depolarization by GABA of rat neostriatum cells *in vitro*. *Exp Brain Res* 45:108–114.
- Momiyama T (2002) Dopamine receptors and calcium channels regulating

- striatal inhibitory synaptic transmission (in Japanese). *Nippon Yakurigaku Zasshi* 120:61P–63P.
- Murer MG, Tseng KY, Kasanetz F, Belluscio M, Riquelme LA (2002) Brain oscillations, medium spiny neurons, and dopamine. *Cell Mol Neurobiol* 22:611–632.
- Nadjar A, Brotchie JM, Guigoni C, Li Q, Zhou SB, Wang GJ, Ravenscroft P, Georges F, Crossman AR, Bezard E (2006) Phenotype of striatofugal medium spiny neurons in parkinsonian and dyskinetic nonhuman primates: a call for a reappraisal of the functional organization of the basal ganglia. *J Neurosci* 26:8653–8661.
- Nicola SM, Surmeier J, Malenka RC (2000) Dopaminergic modulation of neuronal excitability in the striatum and nucleus accumbens. *Annu Rev Neurosci* 23:185–215.
- Nowak L, Bregestovski P, Ascher P, Herbet A, Prochiantz A (1984) Magnesium gates glutamate-activated channels in mouse central neurones. *Nature* 307:462–465.
- Plenz D, Aertsen A (1996) Neural dynamics in cortex-striatum co-cultures—II. Spatiotemporal characteristics of neuronal activity. *Neuroscience* 70:893–924.
- Plenz D, Kitai ST (1998) Up and down states in striatal medium spiny neurons simultaneously recorded with spontaneous activity in fast-spiking interneurons studied in cortex–striatum–substantia nigra organotypic cultures. *J Neurosci* 18:266–283.
- Raz A, Feingold A, Zelanskaya V, Vaadia E, Bergman H (1996) Neuronal synchronization of tonically active neurons in the striatum of normal and parkinsonian primates. *J Neurophysiol* 76:2083–2088.
- Steidl EM, Neveu E, Bertrand D, Buisson B (2006) The adult rat hippocampal slice revisited with multi-electrode arrays. *Brain Res* 1096:70–84.
- Sullivan MA, Chen H, Morikawa H (2008) Recurrent inhibitory network among striatal cholinergic interneurons. *J Neurosci* 28:8682–8690.
- Surmeier DJ, Kitai ST (1993) D1 and D2 dopamine receptor modulation of sodium and potassium currents in rat neostriatal neurons. *Prog Brain Res* 99:309–324.
- Taverna S, Canciani B, Pennartz CM (2007) Membrane properties and synaptic connectivity of fast-spiking interneurons in rat ventral striatum. *Brain Res* 1152:49–56.
- Taverna S, Ilijic E, Surmeier DJ (2008) Recurrent collateral connections of striatal medium spiny neurons are disrupted in models of Parkinson's disease. *J Neurosci* 28:5504–5512.
- Tepper JM, Bolam JP (2004) Functional diversity and specificity of neostriatal interneurons. *Curr Opin Neurobiol* 14:685–692.
- Tepper JM, Wilson CJ, Koós T (2008) Feedforward and feedback inhibition in neostriatal GABAergic spiny neurons. *Brain Res Rev* 58:272–281.
- Tseng KY, Kasanetz F, Kargieman L, Riquelme LA, Murer MG (2001) Cortical slow oscillatory activity is reflected in the membrane potential and spike trains of striatal neurons in rats with chronic nigrostriatal lesions. *J Neurosci* 21:6430–6439.
- Tunstall MJ, Oorschot DE, Kean A, Wickens JR (2002) Inhibitory interactions between spiny projection neurons in the rat striatum. *J Neurophysiol* 88:1263–1269.
- Tyzio R, Ivanov A, Bernard C, Holmes GL, Ben-Ari Y, Khazipov R (2003) Membrane potential of CA3 hippocampal pyramidal cells during postnatal development. *J Neurophysiol* 90:2964–2972.
- Venance L, Glowinski J, Giaume C (2004) Electrical and chemical transmission between striatal GABAergic output neurones in rat brain slices. *J Physiol* 559:215–230.
- Verheugen JA, Fricker D, Miles R (1999) Noninvasive measurements of the membrane potential and GABAergic action in hippocampal interneurons. *J Neurosci* 19:2546–2555.
- Wilson CJ (2007) GABAergic inhibition in the neostriatum. *Prog Brain Res* 160:91–110.
- Wilson CJ, Groves PM (1980) Fine structure and synaptic connections of the common spiny neuron of the rat neostriatum: a study employing intracellular inject of horseradish peroxidase. *J Comp Neurol* 194:599–615.
- Wilson CJ, Kawaguchi Y (1996) The origins of two-state spontaneous membrane potential fluctuations of neostriatal spiny neurons. *J Neurosci* 16:2397–2410.
- Zhou FM, Wilson CJ, Dani JA (2002) Cholinergic interneuron characteristics and nicotinic properties in the striatum. *J Neurobiol* 53:590–605.